Power Performance and Application to Monitoring

Patrick Milan, Matthias Wächter and Joachim Peinke

published in

Handbook of Wind Power Systems, eds.: Panos M. Pardalos, Mario V. Pereira, Niko A. Iliadis, Steffen Rebennack, Nikita Boyko (Springer 2014) 673-708

Abstract The concept of power performance is introduced as the ability of a wind turbine to extract power from the wind. The general performance estimates such as the power coefficient or the theoretical power curve are introduced in laminar conditions. Following Betz' limit, an upper limit for the power available in the wind is derived, as well the main sources of energy loss.
This laminar theory is too simple to describe operating wind turbines, and turbulent and atmospheric effects call for statistical tools. An IEC norm defines the international standard to measure and analyze power performance. The resulting IEC power curve gives a first estimation, and can be used to evaluate the annual energy production. An alternative is proposed with the Langevin power curve, which quantifies the high-frequency dynamics of a wind turbine power production to changing wind speeds. This brings further insight on the overall performance, and allows for applications such as performance monitoring or power modeling.

1 Introduction

The only purpose of a wind power system is to extract energy from the wind. From this statement, building wind turbines might sound like an outdated challenge. The first designs were successfully developed in the Antiquity to provide mechanical

M. Sc. Patrick Milan
ForWind - Center for Wind Energy Research of the Universities of Oldenburg, Hannover and Bremen, Oldenburg, Germany, e-mail: patrick.milan@forwind.de

Dr. Matthias Wächter
ForWind - Center for Wind Energy Research of the Universities of Oldenburg, Hannover and Bremen, Oldenburg, Germany, e-mail: matthias.waechter@forwind.de

Prof. Dr. Joachim Peinke
ForWind - Center for Wind Energy Research of the Universities of Oldenburg, Hannover and Bremen, Oldenburg, Germany, e-mail: joachim.peinke@forwind.de

energy around the globe. The integration of the first wind turbines into electrical networks goes back to the late 19^{th} century, soon after the first power lines were erected. Wind energy is one of the oldest sources of energy. Despite a long history, it remains relatively poorly understood. While its industry recently entered a new age of its evolution, raise more questions and challenges. Before understanding fully how to harness the wind, it is necessary to understand how the wind works. The staggering level of complexity of turbulent and atmospheric effects accounts for many of the remaining challenges that encounters the wind energy industry.

Besides the technical challenge of designing and building rotating machines over 100 meters in diameter, must be considered their integration into a turbulent, ever-changing wind flow. While the wind *signal* that can feel a wind turbine displays complex statistics, its mechanical extraction and transformation into electrical energy adds to the complexity. This justifies why it is so difficult to define unambiguously power performance for wind power systems. A basic theory was developed, that sets aside the turbulent fluctuations, following Betz' developments from the 1920's. This represents the main focus of section 2. Besides giving a good first estimation, this *laminar* theory remains unrealistic to solve the current challenges. More recently, statistical tools were developed in order to integrate the features of turbulence into a more realistic theory of power performance, as introduced in section 3. Although these tools represent large simplifications of the actual dynamics of a wind turbine, they bring useful insights for various applications. An overview of some central applications is introduced in section 4, such as prediction of annual energy production or dynamical monitoring.

This chapter is titled *Power Performance and Application to Monitoring*. Most of its content is oriented towards an introduction to power performance. Power performance is a central aspect of wind energy, and somehow carries its own interest. But it is in its applicability that lies its central interest. Uncomplicated quantities like the power coefficient or power curves are the main estimates of the global *health* of a wind turbine, and can serve as simplified mathematical models. Such models as those introduced in this chapter, although very general and unspecialized, can assist more exclusive applications like monitoring, power prediction or grid integration, that remain in essence very specialized topics. This sets the direction, in between physics and wind power systems, away from dedicated applications but always in connection with them, towards a better understanding of the wind and how to harness it.

2 Power performance theory

This section presents the concept of power performance for wind turbines, starting from momentum theory to power curves. It is meant to give an introduction to the underlying theory, before applications are presented in sections 3 and 4. While this chapter deals only with horizontal-axis three-bladed electrical wind turbines, there is no major limitation to its extension to other designs of wind power systems.

2.1 Momentum theory for wind turbines

In this section 2.1, a basic understanding of fluid mechanics will be applied to wind turbines. For a more detailed description on momentum theory, the reader is kindly referred to [6]. This theoretical approach sets ground for the further power curve analysis. The complexity of turbulence is first set aside, so as to understand the fundamental behavior of a wind turbine in a uniform flow at steady-state. More complex atmospheric effects represent active research topics, whose detailed analysis is outside the scope of this introduction, cf. [5].

As a wind turbine converts the power from the wind into available electrical power, one can assume the following relation

$$P(u) = c_p(u) \times P_{wind}(u)\,, \tag{1}$$

where $P_{wind}(u)$ is the power contained in the wind passing with speed u through the wind turbine, and $P(u)$ is the electrical power extracted. The amount of power converted by the wind turbine is given by the so-called power coefficient $c_p(u)$, which represents the efficiency of the machine. As the input $P_{wind}(u)$ cannot be controlled, improving power performance means increasing the power coefficient $c_p(u)$. The power contained in a laminar incompressible flow moving along the $x-axis$ with constant speed u through a vertical plane of area A is

$$\begin{aligned} P_{wind}(u) &= \frac{d}{dt}E_{kin,wind} = \frac{d}{dt}\left(\frac{1}{2}mu^2\right) \\ &= \frac{1}{2}\frac{dm}{dt}u^2 = \frac{1}{2}\frac{d(\rho V)}{dt}u^2 \\ &= \frac{1}{2}\rho\frac{d(Ax)}{dt}u^2 = \frac{1}{2}\rho A u^3\,. \end{aligned} \tag{2}$$

Let us consider a mass of air moving towards a wind turbine, which can be represented by an actuator disc[1] of diameter D. When crossing the wind turbine, the wind is affected as parts of its energy is extracted. This extraction of kinetic energy results in a drop in the wind speed from upstream to downstream. The velocity far before the wind turbine (upstream), at the wind turbine and far behind (downstream) are labelled respectively u_1, u_2 and u_3. An illustration is given in Fig. 1, see also [6].

Mass conservation requires that the flow-rate $\dot{m} = A_i\rho u_i$ be conserved and

$$A_1\rho u_1 = A_2\rho u_2 = A_3\rho u_3\,, \tag{3}$$

where A_i are the respective areas perpendicular to the flow. A_2 is the area swept by the rotor blades $A_2 = A = \pi D^2/4$. As a consequence of the wind speed slowing

[1] An actuator disc is an infinitely thin disc through which the air can flow without resistance, as proposed by Froude and Rankine's momentum theory [13].

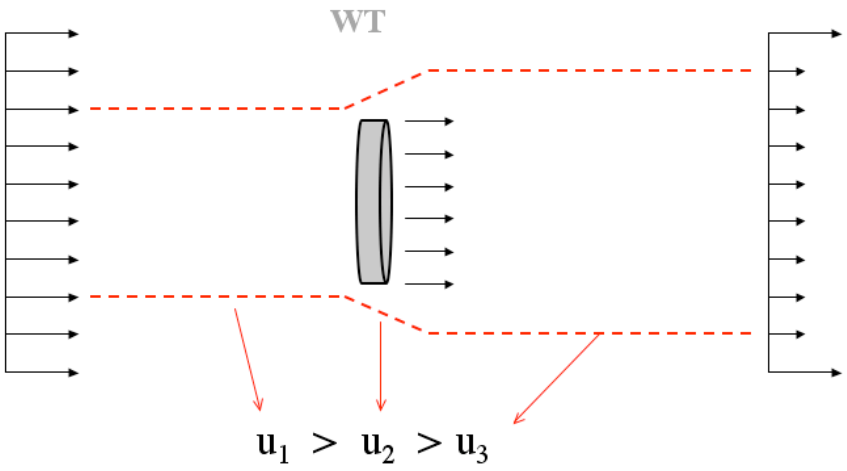

Fig. 1 Idealized flow situation around a wind turbine (WT) according to [21]. The wind speeds before, at and after the wind turbine are respectively u_1, u_2 and u_3.

down, i.e. $u_3 < u_2 < u_1$, the area of the stream-tube[2] has to expand, and $A_3 > A_2 > A_1$. This can be observed in Fig. 1.

Also, the energy extracted by the wind turbine can be determined by the difference of kinetic energy upstream and downstream of the wind turbine

$$E_{ex} = \frac{1}{2} m(u_1^2 - u_3^2)\,, \tag{4}$$

resulting in a power extraction

$$P_{ex} = \frac{d}{dt} E_{ex} = \frac{1}{2} \dot{m}(u_1^2 - u_3^2)\,. \tag{5}$$

The wind power cannot be totally converted into mechanical power because the wind turbine continuously takes energy out of the wind flow, which reduces its velocity. However, the flow needs to *escape* the wind turbine downstream with a speed $u_3 > 0$. If all the power content of the wind would be extracted, the wind speed downstream would then become zero. As a consequence, the air would *accumulate* downstream and block newer air from flowing through the wind turbine, so that no more power could be extracted. This means that the wind flow must keep some energy to escape, which naturally sets a limit for the efficiency of any wind power system. The power coefficient $c_p(u)$ must be inferior to 1. An optimal ratio of wind speeds $\mu = u_3/u_1$ can be found that allows for the highest energy extraction, as introduced in section 2.2.

[2] A stream-tube is defined here as the stream of air particles that interact with the wind turbine.

2.2 Power performance

In the plane of the rotor blades, an intermediate value of wind speed

$$u_2 = \frac{u_1 + u_3}{2} \tag{6}$$

is found[3]. Knowing this value one also knows the flow-rate in the rotor plane area that is now given by

$$\dot{m} = \rho A u_2 \,. \tag{7}$$

Inserting equations (6) and (7) into equation (5) yields

$$\begin{aligned} P(\mu) &= \frac{1}{2}\rho A u_1^3 \times \frac{1}{2}(1+\mu-\mu^2-\mu^3) \\ &= P_{wind}(u_1) \times c_p(\mu) \,. \end{aligned} \tag{8}$$

The theoretical definition of the power coefficient is then

$$c_p(\mu) = \frac{1}{2}(1+\mu-\mu^2-\mu^3)\,, \tag{9}$$

where $\mu = u_3/u_1$, as shown in Fig. 2. The optimal power performance is obtained

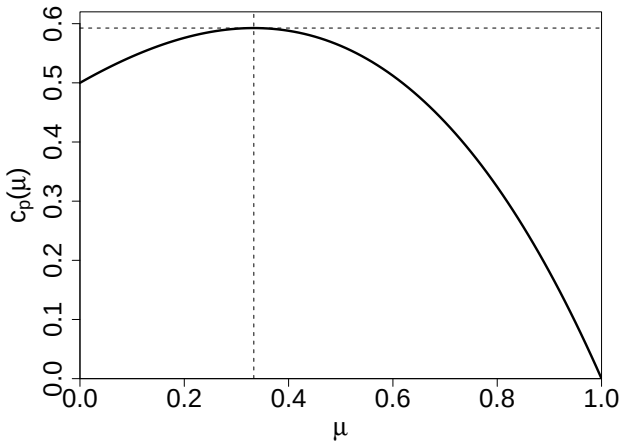

Fig. 2 Power coefficient c_p as a function of the wind speed ratio $\mu = u_3/u_1$.

for a ratio μ such that the derivative of $c_p(\mu)$ with respect to μ is zero

[3] Following Froude-Rankine, it can be shown that this value is the optimal value.

$$\frac{d}{d\mu}c_p(\mu) = \left(-\frac{1}{2}\right) \times \left(3\mu^2 + 2\mu - 1\right) = 0\,. \tag{10}$$

This leads to $\mu_{max} = 1/3$ and a corresponding $C_p(\mu_{max}) = 16/27 \approx 0.593$, as shown in Fig. 2.

This limit is called the Betz limit, as it was found by Albert Betz in 1927 [2]. In other words, a wind turbine can extract at most 59.3% of the power contained in the wind. This can be obtained when the wind speed downstream is one-third of the wind speed upstream.

A widely used representation of power performance is given by the relation of c_p to the tip speed ratio λ defined as

$$\lambda = \frac{\omega R}{u_1}\,, \tag{11}$$

where ω and R are the angular frequency and radius of the rotor. λ is the ratio of the rotational speed at the tip of the blades to the upstream wind speed. The dimensionless $c_p - \lambda$ curve is introduced in section 2.3.

Betz' momentum theory only considers the mechanical transfer of energy from the wind to the rotor blades. The next step of the conversion from mechanical to electrical energy has not been taken into account, as well as all energy losses. The more complex design of wind turbines causes lower values of c_p, as discussed in section 2.3. The power coefficients of modern commercial wind turbines reach values of order 0.5. Also, criticism of Betz theory is given in [14, 15], leading to a less well defined upper limit of c_p.

2.3 Limitations of Betz theory - energy losses

Although it is based on a simplified approach, the Betz limit is a widely used and accepted value. But more realistic considerations indicate that real wind turbine designs have even lower efficiency due to additional limitations. In this section, the three main limitations to reach the optimal value of $c_p = 16/27$ are introduced. Additional considerations, e.g. the finite number of blades and losses due to the drag and stall effects on the blades are discussed in [6, 3]. All the derivations introduced in this section 2.3 are based on appendix 6. This section only aims to give a first idea. For a more detailed understanding of the mathematical equations presented here, the reader is kindly referred to the appendix first.

2.3.1 Bouncing losses

Betz' consideration does not take into account that there is not only a reduction of wind speed downstream, but also an additional angular momentum that is transferred to the air flow, as shown in Fig. 3.

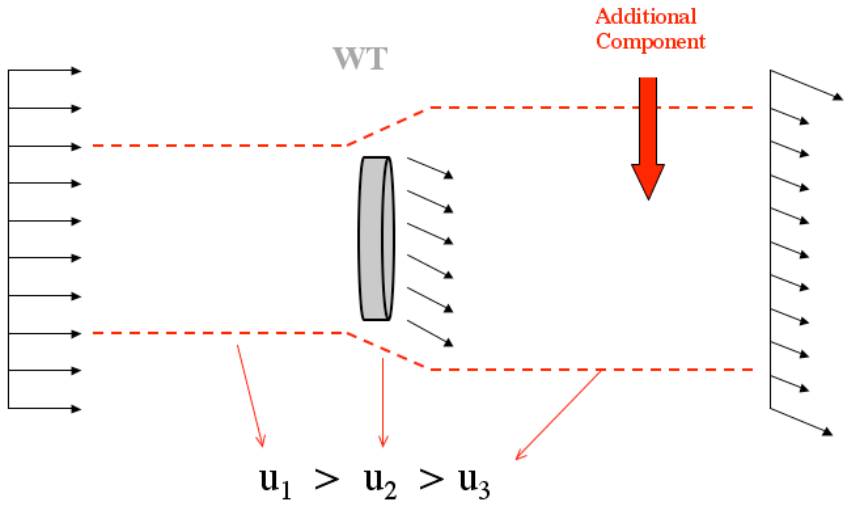

Fig. 3 Flow around a wind turbine. After passing the turbine the velocity field has a rotational component due to the rotating rotor blades.

This effect follows Newton's third law, as a reaction to the rotational motion of the rotor. The energy loss is more important for smaller tip speed ratios, following a derivation in appendix 6. This follows equation (36) where a small velocity ωr requires a larger force F_r (the subscript $_r$ indicates the rotational direction) to obtain the same power. So for slow rotating wind turbines (λ small), these losses are much more severe than for fast rotating machines. For instance, for $\lambda \approx 1$ an optimum value of c_p of only 0.42 can be reached instead of the Betz optimum of 0.59. c_p approaches the Betz optimum with increasing tip speed ratio.

2.3.2 Profile losses

Another important source of energy loss is the quality of the airfoil profile. According to equations (33) and (36) in appendix 6, a cut dr at radius r yields a power extraction

$$dP = z\omega r\frac{\rho}{2}c^2 \times t \times dr\left[(C_L cos(\beta) - C_D sin(\beta)\right] . \tag{12}$$

For a perfect (ideal) airfoil the drag vanishes and

$$dP_{ideal} = z\omega r\frac{\rho}{2}c^2 \times t \times dr \times C_L cos(\beta)\,. \tag{13}$$

The efficiency η can now be defined as the ratio between equation (12) and equation (13), i.e. dP/dP_{ideal}. The general definition of the efficiency is given by

$$\eta = 1 - \xi\,. \tag{14}$$

The profile losses ξ_{prof} follow the relation

$$\xi_{prof} \propto r\lambda\,. \tag{15}$$

In contrast to the bouncing losses, the profile losses mainly affect fast rotating machines. For higher tip speed ratios, the lift to drag ratio C_L/C_D must be optimized. Furthermore the losses increase with the radius, such that the manufacturing quality of the blade tips is of primary importance for power performance.

2.3.3 Tip losses

A good quality of the tips especially means that they should be as narrow as possible because this corresponds to an (ideal) airfoil with length infinity ($R/t = \infty$). For real blades there is always a flow around the end of the blade (forming an eddy that is advected by the flow) from the high pressure area to the low pressure area. This is partly levelling the pressure difference and consequently the lift force. The tip losses obey approximately the following relation

$$\xi_{tip} \propto \frac{1}{z\lambda}. \tag{16}$$

Different to the profile losses an increasing tip speed ratio decreases the tip losses, as well as an increased number of blades.

2.3.4 Impact on power performance

Fig. 4 shows an overview of the different kinds of losses and their influence on the value of c_p. One can see that bouncing losses cause the largest reduction in the power coefficient for small values of λ, similar to the finite number of blades. This is the opposite for the profile losses. Three-bladed wind turbines can reach optimal c_p values of order 0.50 for typical values of $\lambda \approx 6-8$, which naturally sets the strategy for optimal power performance in terms of rotational frequency ω.

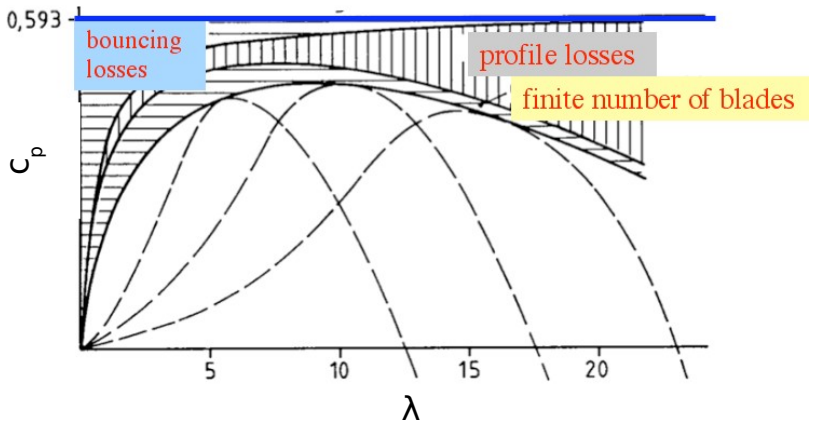

Fig. 4 Illustration of the influence of different sources of energy loss on the efficiency of a wind turbine.

2.4 Theoretical power curve

Along with the $c_p - \lambda$ curve, a standard representation of a wind turbine power performance is given by a so-called power curve. The power curve gives the relation between the simultaneous wind speed u and power output P. Following usual practice, the wind speed u will refer to the upstream horizontal wind speed u_1 from now on (such that $u = u_1$). Also, the net electrical power output P that the wind turbine actually delivers to the grid is considered, integrating all possible losses. The two quantities u and P will follow these specifications until the end of the chapter. Following equation (8), the theoretical power curve reads

$$\begin{aligned} P(u) &= c_p(u) \times P_{wind}(u) \\ &= c_p(u) \times \tfrac{1}{2}\rho A u^3 \,. \end{aligned} \tag{17}$$

In most of the modern wind turbine designs, the regulation of the power output is performed through changes both in the rotational frequency of the generator and in the pitch angle of each blade[4]. The rotational frequency of the generator is physically linked to the wind speed, such that it cannot be changed freely. However, the pitch angle of the blades can be controlled at will, and almost independently of the wind speed, to reach the chosen control strategy, and hence represents the central mean of control for the operation. Pitching plainly consists of a rotation of the

[4] Other wind turbine designs involve fixed rotational frequency (called fixed-speed wind turbines) or fixed pitch angle (called fixed-pitch wind turbines). A more detailed description on control strategies is given in [3].

blades by a pitch angle θ in the plane of their cross-section. We will refer only to this design in this section 2.4.

The power production is then controlled by changing the lift forces on the rotor blades [6, 3]. The power production can be reduced or stopped by pitching the blades towards stall[5]. In modern wind turbines, this is achieved by a so-called active pitch control. The power coefficient c_p depends strongly on this pitch angle θ and on the tip speed ratio λ, i.e. $c_p = c_p(\lambda(u), \theta)$. As λ can typically not be controlled, c_p is optimized via θ to a desired power production. In particular for high wind speeds, c_p is lowered to protect the wind turbine machinery and prevent from overshoots in the power production.

This pitch regulation is commanded by the controller of the wind turbine, which constitutes of several composite mechanical-electrical components that operate actively for the optimum power performance[6]. For the common pitch-controlled wind turbines, the control strategy gives four distinct modes of operation:

- for $u \leq u_{cut-in}$,[7] the power contained in the wind is not sufficient to maintain the wind turbine into motion, and no power is produced;
- in partial load $u_{cut-in} \leq u \leq u_r$,[8] the wind turbine works at its maximum power performance, i.e. c_p is maximized, and the pitch angle θ is normally maintained constant;
- in full load $u_r \leq u \leq u_{cut-out}$, [9] the wind turbine power output is limited to the rated power P_r. In this mode of operation, the pitch angle θ is adjusted in real-time to maintain $P \approx P_r$;
- for $u > u_{cut-out}$ the pitch angle θ is maximized to the feathered position so as to eliminate the lift forces on the blades. A braking device can be used in addition to block the rotation for safety reasons. As a consequence, the power production is stopped.

An illustration of the theoretical strategy for $c_p(u)$ and $P(u)$ is given in Fig. 5.

It is important to precise that this theoretical estimation is valid for a laminar flow, which never occurs in real situations. The more complex atmospheric winds call for more complex descriptions of power performance. Following the path of turbulence research, statistical models are introduced in section 3 to deal with this complexity.

[5] Stall effects are obtained when the angle of attack of an airfoil exceeds a critical value, resulting in a sudden reduction in the lift force generated. A detailed study on airfoil lift effects can be found in [20].

[6] Additional considerations such as mechanical loads or power stability are usually taken into account as well [3], but reach out of the scope of this chapter.

[7] u_{cut-in} represents the minimum wind speed such that the wind turbine can extract power, typically in the order of $3-4m/s$.

[8] u_r represents the rated wind speed at which the wind turbine extracts the rated, maximum allowed power P_r, typically in the order of $12-15m/s$.

[9] $u_{cut-out}$ represents the maximum wind speed at which the wind turbine can safely extract power, typically in the order of $25-35m/s$.

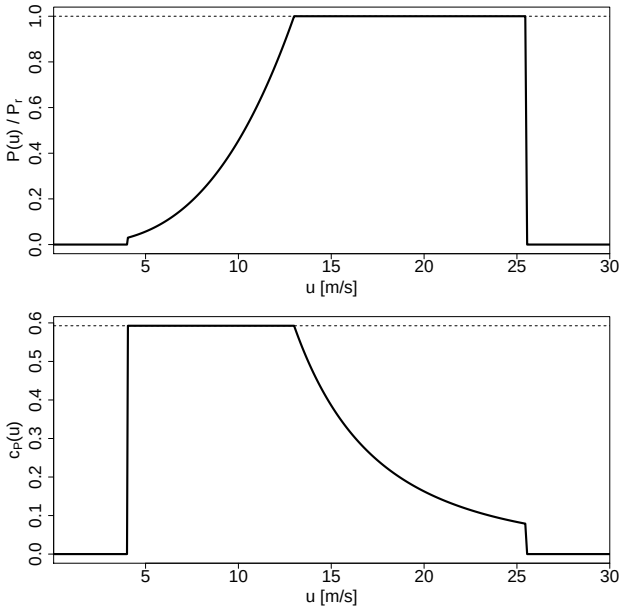

Fig. 5 (a) Theoretical power curve $P(u)$; (b) Theoretical power coefficient $c_p(u)$ for a pitch-controlled wind turbine with $u_{cut-in} = 4$ m/s, $u_r = 13$ m/s and $u_{cut-out} = 25$ m/s.

3 Application to operating wind turbines

The theory of wind power performance was introduced in section 2. Although this theory sets a good foundation for wind energy applications, the complexity of atmospheric effects calls for a more advanced description. This section 3 presents the typical complex data of wind speed u and power output P recorded on wind turbines in section 3.1. It is followed by two approaches to estimate power curves in sections 3.2 and 3.3, respectively the IEC and the Langevin procedures.

For information, all the results presented were derived from measurements on operating multi-MW commercial wind turbines, with a sampling frequency 1Hz (unlike stated otherwise). All power values are normalized by the rated power P_r in order not to confuse the reader. All results can straightforwardly be converted back to actual power values.

3.1 Atmospheric turbulence - a complex challenge

The introduction in section 2 assumed a steady, laminar wind inflow $\mathbf{u_1} = \mathbf{constant}$. Although it is a necessary assumption to derive Betz limit, atmospheric flows are turbulent. Atmospheric winds combine the complex aspects of turbulence on small scales and of climatology on larger scales. The statistics of wind measurements display complex properties like unstationarity or intermittency (such as gusts). An illustration on wind statistics is presented here, as well as their impact on power output statistics.

Two typical time series for the simultaneous measurement of wind speed u and power output P are displayed in Fig. 6 and 7. The ten-minute average and standard deviation are displayed, illustrating how the IEC norm reduces the complexity of the measurement signals (see section 3.2).

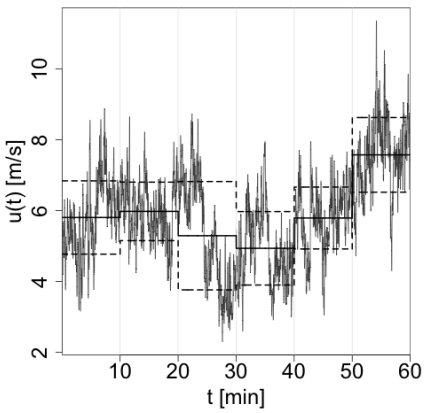

Fig. 6 Excerpt of a wind speed measurement at frequency 1Hz for one hour. The ten-minute average and standard deviation are displayed respectively with the solid and dashed lines.

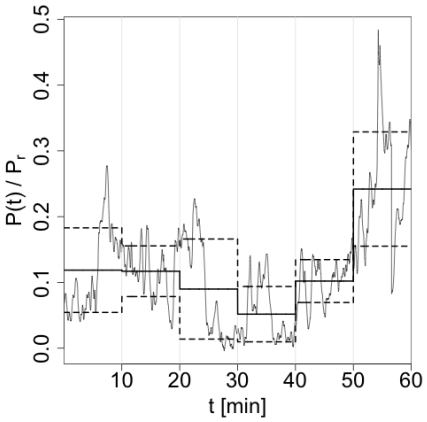

Fig. 7 Excerpt of a power output measurement at frequency 1Hz for one hour. The ten-minute average and standard deviation are displayed respectively with the solid and dashed lines.

The time series can be plotted together, i.e. power output versus wind speed for the same measurement, as shown in Fig. 8.

One can see from Fig. 8 that when no time-averaging is performed, the power conversion is a highly dynamical system even on very short time scales. The power signal reacts quickly to the wind speed signal, and can be considered *turbulent* as well. An important aspect for the wind energy industry is the impact of gusts[10] on wind turbines fatigue loads, as well as on power stability. Gusts can be estimated from the statistics of the increments of wind speed

[10] Although no unique, clear definition of gust exists, one can see a wind gust as a rapid change of wind speed (and possibly direction). Gusts are *extreme events*.

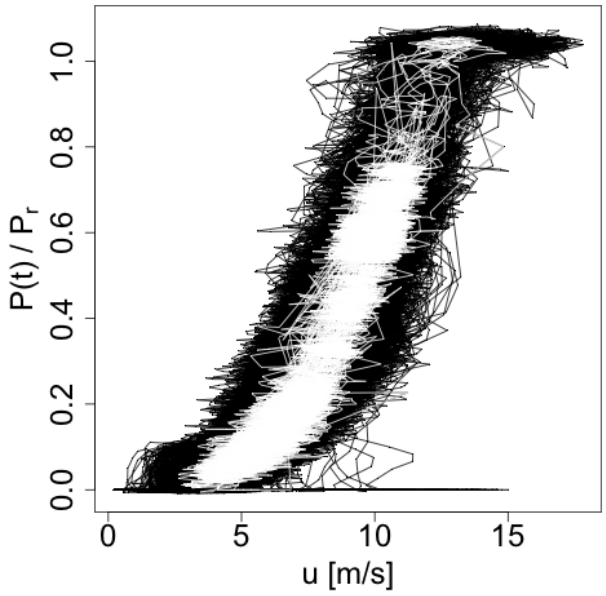

Fig. 8 1Hz measurement of power output versus wind speed during 10^6 sec. The data is plotted in black for the first 960.000 points, then in white for the last 40.000 points.

$$u_\tau(t) = u(t+\tau) - u(t)\,, \tag{18}$$

where τ is the time increment, or scale of interest. $u_\tau(t)$ then represents the change in wind speed between time t and time $t+\tau$. Similarly, the increments of power output can be defined as

$$P_\tau(t) = P(t+\tau) - P(t)\,. \tag{19}$$

Following what is usually done in research on turbulence, the probability density function (PDF) of u_τ is displayed in Fig. 9, as well as the PDF of P_τ in Fig. 10. For information, the increments are systematically normalized by their standard deviation σ_τ, such that only the shape of the PDF is of interest.

Compared to a normal, i.e. Gaussian distribution, the normalized PDFs of u_τ and P_τ can be seen as intermittent[11], especially for the short time scales $\tau \approx 1 - 100$ sec. The PDFs are most intermittent for small values of τ, indicating that the intermittent dynamics act on short time scales. This means that the probability of sustaining a major change of wind speed or power output is higher over short time

[11] The notion of intermittency is related to the probability of a process to sustain extreme events. It can be identified as a large deviation from the Gaussian distribution far away from the mean value. Extreme events such as gusts yield intermittent PDFs.

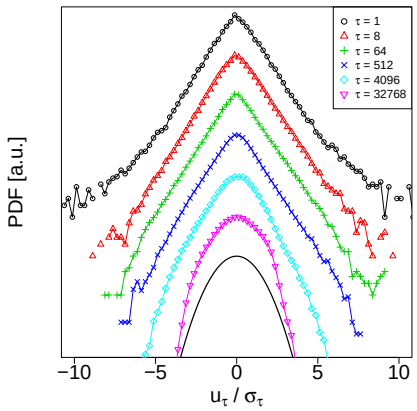

Fig. 9 PDF of normalized wind speed increments for various time increments τ (increasing τ downwards). The values of τ are given in seconds. The various PDFs are intentionally shifted vertically for clarity. A Gaussian distribution is given as a reference (solid line).

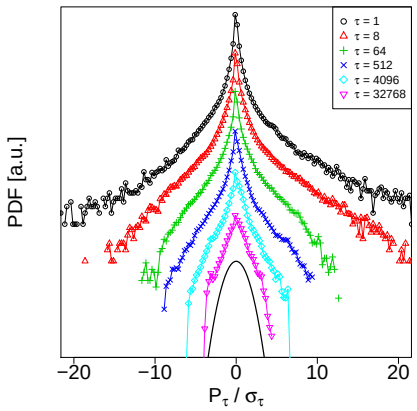

Fig. 10 PDF of normalized power output increments for various time increments τ (increasing τ downwards). The values of τ are given in seconds. The various PDFs are intentionally shifted vertically for clarity. A Gaussian distribution is given as a reference (solid line).

intervals. When increasing the scale τ, the increment PDFs of u and P then become less intermittent and tend towards the Gaussian distribution[12].

While this is a well-known result for turbulent winds [5], this aspect is seldom emphasized for wind turbines power output, see [8].

The information displayed in Fig. 10 is important to understand wind turbines behavior and for the wind energy industry in general, as it shows a non-zero probability of having extreme changes in power output. For example for $\tau =$ 64 sec, events $P_\tau \approx 10\sigma_\tau \approx 0.75P_r$ were recorded, meaning that the power output can increase by about 75% of the rated power within a minute. Also for $\tau = 8$ sec, events $P_\tau \approx 20\sigma_\tau \approx 0.6P_r$ occur, meaning that the power output can increase by about 60% of the rated power within 8 seconds.

PDFs of power output increments appear to be even more intermittent than PDFs of wind speed increments. This can be justified by the cubic relation of the power output to the wind speed. As a matter of fact, when the wind speed doubles, the power output should theoretically increase by a factor 8. This justifies why wind gusts are transferred and amplified to the power production which, as a consequence, suffers rapid changes relatively often. This certainly accounts for the shorter lifetime of wind turbines than originally designed. Also, these rapid changes in power pro-

[12] Following the central-limit theorem, the PDF of a large-enough dataset of independent, random samples approaches the Gaussian distribution [12].

duction are fed into the grid, and raise the matter of the power stability for wind energy integration.

3.2 The international standard: the IEC power curve

The standard power performance procedure for wind turbines was defined by the International Electrotechnical Commission in 2005 in the norm IEC 61400-12-1. For a detailed description of this norm, the reader is kindly referred to the complete proceeding [10]. This procedure provides a unique methodology to ensure accuracy, consistency and reproducibility in the measurement and in the analysis of power performance. It consists first of the minimum requirements for a power performance test, and second of a procedure to process the measured data without extensive knowledge.

3.2.1 Measurement procedure

First, are described the necessary preparations for the performance test, such as criteria for the measurement equipments, guidance for the location and setup of the meteorological mast that will be used to measure the wind speed and other parameters like the wind direction, temperature and air pressure. The sector of the measurement is also described as the range of wind directions that are valid for a representative measurement, such that wind directions where the met mast is in the wake of the wind turbine must be excluded. A detailed assessment of the terrain at the test site is presented in the additional site calibration procedure which reports for additional obstacles (other than the wind turbine).

The first goal of the IEC norm is to ensure that the data collection displays a sufficient quantity and quality for an accurate estimation of the power performance.

3.2.2 IEC power curve

Second, the measured data is processed[13]. The data processing is mainly performed in two steps.

[13] Additional correction of the measured data should be performed using temperature and pressure measurements.

After adequate normalization of the data, the first step consists in averaging the measured data over time intervals of 10 minutes. The IEC power curve is derived in a second step from the ten-minute averages using the so-called method of bins, i.e. the data is separated into wind speed intervals of width 0.5 m/s.

In each interval i, bin averages of wind speed u_i and power output P_i are calculated according to

$$u_i = \frac{1}{N_i} \sum_{j=1}^{N_i} u_{norm,i,j} \quad , \quad P_i = \frac{1}{N_i} \sum_{j=1}^{N_i} P_{norm,i,j} \,, \tag{20}$$

where $u_{norm,i,j}$ and $P_{norm,i,j}$ are the normalized 10-minute average values of wind speed and power, and N_i is the number of 10 min data sets in the i^{th} bin.

For the power curve to be complete and reliable, each wind speed bin must include at least 30 minutes of sampled data. Also, the total measurement time must cover at least a period of 180 hours. The range of wind speeds must range from 1 m/s below cut-in wind speed to 1.5 times the wind speed at 85% of the rated power of the wind turbine. The norm also provides an estimation of uncertainty as the standard error of the normalized power data, plus additional uncertainties related to the instruments, the data acquisition system and the surrounding terrain. A typical IEC power curve is presented in Fig. 11.

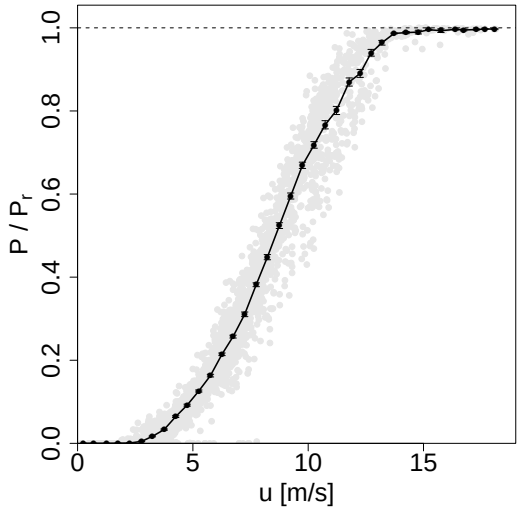

Fig. 11 Power curve (black line with corresponding error bars) obtained according to the IEC norm. The grey dots represent the 10-minute average values.

The IEC norm also defines the AEP (Annual Energy Production), as presented in section 4.2. The AEP is a central feature for economical considerations, as it gives a first estimate of the long-time energy production of a wind turbine. As it sets a unique ground for wind power performance worldwide, the IEC norm helps building a general understanding between manufacturers, scientists and end-users. This statement comes to be ever more important as the wind energy sector grows. Hence, focusing on this standard is paramount to any study on power performance.

3.2.3 Turbulence-induced deviations

As a downside to its simplicity, the IEC power curve method presents a limitation. In contrast to a good definition of the requirements in section 3.2.1, the definition of the power curve in section 3.2.2 suffers a mathematical imperfection. In order to deal with the complexity of the wind speed and power signals, the data is systematically averaged over time. Although a statistical averaging is necessary to extract the main features from the complex processes, the averaging procedure over 10-minute intervals lacks a clear physical meaning, beyond its statistical definition. As the wind[14] fluctuates on various time scales (down to seconds and less), a systematic averaging over ten minutes filters out all the short-scale turbulent dynamics. Combining these turbulent fluctuations with the non-linear power curve $P(u) \propto u^3$, the resulting IEC power curve is spoiled by mathematical errors. To show this, one can first split the wind speed $u(t)$ sampled at 1Hz into its mean value and the fluctuations around this mean value

$$u(t) = \overline{u(t)} + u'(t)\,, \tag{21}$$

where $\overline{x(t)}$ represents the average (arithmetic mean) value of x. Assuming that $u'(t) \ll \overline{u(t)}$, a Taylor expansion of $P(u(t))$ reads [4]

$$\begin{aligned} P\left(u(t)\right) =& P\left(\overline{u(t)}\right) \\ &+ u'(t)\left(\frac{\partial P(u)}{\partial u}\right)_{u=\overline{u(t)}} \\ &+ \frac{u'(t)^2}{2!}\left(\frac{\partial^2 P(u)}{\partial u^2}\right)_{u=\overline{u(t)}} \\ &+ \frac{u'(t)^3}{3!}\left(\frac{\partial^3 P(u)}{\partial u^3}\right)_{u=\overline{u(t)}} \\ &+ o\left(u'(t)^4\right)\,. \end{aligned} \tag{22}$$

Averaging equation (22) yields

[14] To some extent the power output also fluctuates on short time scales, but its high-frequency dynamics are limited by the inertia of the wind turbine.

$$\begin{aligned}\overline{P(u(t))} =& P\left(\overline{u(t)}\right) \\ &+ 0 \\ &+ \frac{\overline{u'(t)^2}}{2}\left(\frac{\partial^2 P(u)}{\partial u^2}\right)_{u=\overline{u(t)}} \\ &+ \frac{\overline{u'(t)^3}}{6}\left(\frac{\partial^3 P(u)}{\partial u^3}\right)_{u=\overline{u(t)}} \\ &+ o\left(u'(t)^4\right), \end{aligned} \tag{23}$$

because $\overline{u'(t)} = \overline{u(t) - \overline{u(t)}} = 0$. This means that the average of the power is not equal to the power of the average, and must be corrected by the 2^{nd} and 3^{rd}-order terms. As the IEC power curve directly relates the 10-minute averages of wind speed and of power output, it neglects the higher-order terms in the Taylor expansion. The 2^{nd}-order term is the product of the variance $\sigma^2 = \overline{u'(t)^2}$ of u(t)[15] and the second-order derivative of the power curve[16]. This demonstrates that the IEC power curve cannot describe in a mathematically rigorous way the nonlinear relation of power to wind speed when coupled with wind fluctuations (stemming from turbulence), at least not without higher-order corrections.

As a consequence of this mathematical over-simplification, the result depends on the turbulence intensity $I = \sigma/\overline{u}$, so on the wind condition during the measurement [4]. It is illustrated in Fig. 12, where the IEC power curve deviates from the theoretical power curve with increasing turbulence intensity, as predicted by equation (23). As it does not characterize the wind turbine only, but also the measurement condition, raises the question of its reproducibility and stability.

3.3 A new alternative: the Langevin power curve

An alternative to the standard IEC power curve is proposed in this section 3.3. As the IEC norm defines the measurement procedure with relevance (see section 3.2.1), the same conditions will be considered for the Langevin analysis. The difference lies in the different approach to process the measured data.

[15] $\sigma^2 = \overline{(u-\overline{u})^2} = \overline{u'(t)^2}$.

[16] Assuming a cubic power curve $P(u) \propto u^3$, $P(u)$ has non-zero derivatives up to 3^{rd}-order. Moreover, the transition point to rated power may have non-zero derivatives of arbitrary order, see Fig. 12.

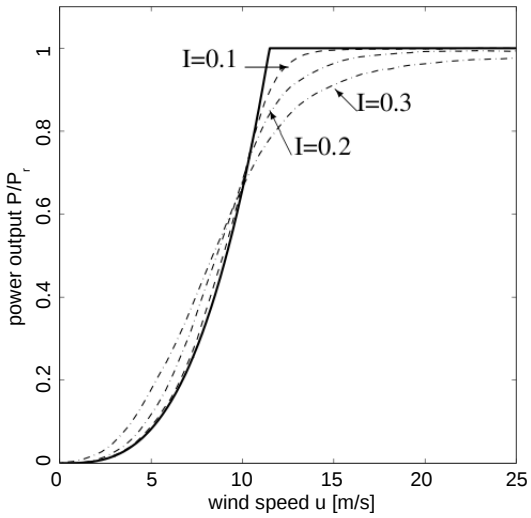

Fig. 12 IEC power curves for various turbulence intensities $I = 0.1,\ 0.2,\ 0.3$ (dashed lines). The full line represents the theoretical power curve. This result was obtained from numerical model simulations from [4].

One additional point on the sampling frequency is however important for the Langevin analysis. Because the method resolves the dynamics of a wind turbine in the order of seconds, a minimum sampling frequency in the order of 1Hz is necessary for the measurements of wind speed and power output.

3.3.1 A dynamical concept

The power characteristic of a wind turbine can be derived from high-frequency measurements without using temporal averaging. One can regard the power conversion as a relaxation process which is driven by the turbulent wind fluctuations [19, 16]. More precisely, the wind turbine is seen as a dynamical system which permanently tries to adapt its power output to the fluctuating wind. For the (hypothetical) case of a laminar inflow at constant speed u, the power output would relax to a fixed value $P_L(u)$[17], as illustrated in Fig. 13. Mathematically, these *attractive* power values $P_L(u)$ are called *stable fixed points* of the power conversion process.

[17] The subscript L stands for "Langevin" as $P_L(u)$ will be associated to the formalism of the Langevin equation.

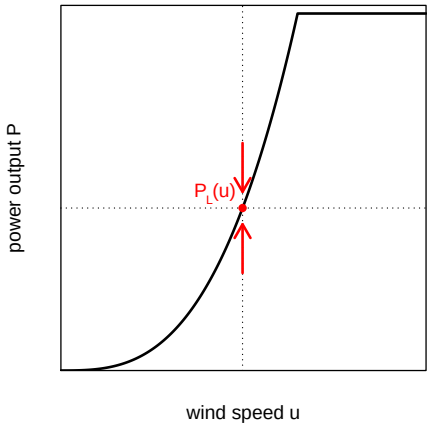

Fig. 13 Illustration of the concept of stable fixed point $P_L(u)$. For constant wind speed, the power output would relax to a stable value $P_L(u)$. This sketch is inspired from [1].

3.3.2 The Langevin equation

The Langevin power curve[18] is derived from high-frequency measurements of wind speed $u(t)$ and $P(t)$. All necessary corrections and normalizations from the IEC norm [10] should be applied on the two time series.

The wind speed measurements are divided into bins u_i of 0.5 m/s width, as done in [10]. This accounts, to some degree, for the non-stationary nature of the wind, yielding quasi-stationary segments $P_i(t)$ for those times t with $u(t) \in u_i$. The following mathematical analysis will be performed on these segments $P_i(t)$. From now on, the subscript $_i$ will be omitted and the term $P(t)$ will refer to the quasi-stationary segments $P_i(t)$. The power conversion process is then modeled by a first-order stochastic differential equation called the Langevin equation[19]

$$\frac{d}{dt}P(t) = D^{(1)}(P) + \sqrt{D^{(2)}(P)} \times \Gamma(t)\,. \tag{24}$$

In this model, the time evolution of the power output is controlled by two terms[20].

$D^{(1)}(P)$ represents the deterministic relaxation of the wind turbine, leading the power output towards the attractive fixed point $P_L(u)$ of the system. For such, $D^{(1)}(P)$ is commonly called the *drift function*.

[18] In former publications on the topic, the Langevin power curve was called *dynamical power curve* or *Markovian power curve*. It is nonetheless the same approach.

[19] This equation is the reason for the name of the Langevin power curve.

[20] $D^{(1)}$ and $D^{(2)}$ are the first two Kramers-Moyal coefficients.

The second term $\sqrt{D^{(2)}(P)} \times \Gamma(t)$ represents the stochastic (random) part of the time evolution, and serves as a simplified model for the turbulent wind fluctuations that drive the system out of equilibrium. The function $\Gamma(t)$ is a Gaussian-distributed, delta-correlated noise with variance 2 and mean value 0. $D^{(2)}(P)$ is commonly called the *diffusion function*. A mathematical approach to the Langevin equation can be found in [18].

3.3.3 The drift function and the Langevin power curve

The deterministic drift function $D^{(1)}(P)$ is of interest as it quantifies the relaxation of the power output towards the stable fixed points of the system. When the system is in a stable state, no deterministic drift occurs[21], and $D^{(1)}(P) = 0$. Following equation (25), $D^{(1)}(P)$ can be understood as the average time derivative of the power signal $P(t)$ in each region of wind speed u_i and power output P.

The drift and diffusion functions can be derived directly from measurement data as conditional moments [18]

$$D^{(n)}(P) = \lim_{\tau \to 0} \frac{1}{n!\tau} \langle (P(t+\tau) - P(t))^n \,|\, P(t) = P \rangle \,, \tag{25}$$

where $n = 1, 2$ respectively for the drift and diffusion functions. The averaging $\langle \cdot \rangle$ is performed over t, as the condition means that the calculation is only considered for those times during which $P(t) = P$.

This means that the averaging is done separately for each wind speed bin u_i and also for each level of the power P. One could speak of a *state-based* averaging on u and P, in contrast to the temporal averaging performed in the IEC norm. A typical drift function is displayed in figure 14.

The dynamics of the power signal can be directly related to the local sign and value of $D^{(1)}$. A positive drift indicates that the power tends to increase (arrows pointing up in Fig. 14), in regions where the wind turbine does not produce enough power for the given wind speed. On the contrary, a negative drift corresponds to a decreasing power (arrows pointing down), in regions where the wind turbine produces too much power for the given wind speed. At the intersection are the points where $D^{(1)} = 0$, indicating that when at this value, the power output is in a stable configuration (the average time derivative is zero). The collection of all the points where the drift function is zero is defined as the Langevin power curve, and will be further labelled $P_L(u)$.

[21] To separate stable (attractive) from unstable (repulsive) fixed points, also the slope of $D^{(1)}(P)$ must be considered.

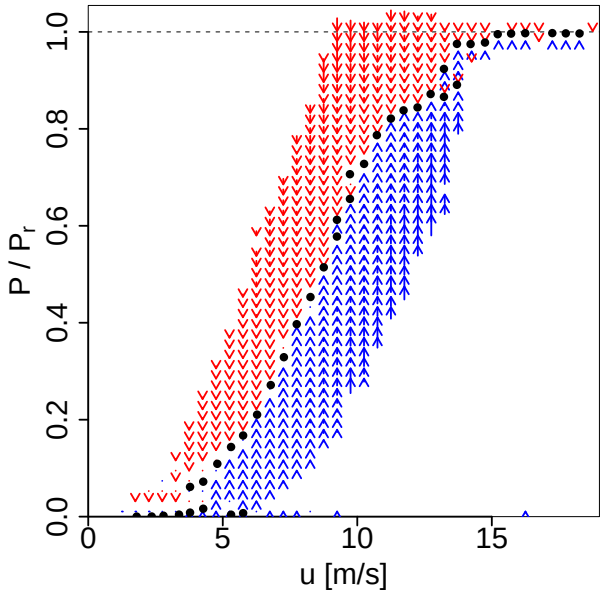

Fig. 14 Drift function $D^{(1)}(P)$. Each arrow represents the local value of $D^{(1)}(P)$ in magnitude (length of the arrow) and direction (pointing up for positive values). The stable fixed points where $D^{(1)}(P) = 0$ are given by the black dots.

The stable fixed points $P_L(u)$ of the power conversion process can be extracted from the measurement data as solutions of

$$D^{(1)}(P_L(u)) = 0\,. \tag{26}$$

An illustration is given in Fig. 15.

Following the mathematical framework of equations (24) and (25), an estimation of uncertainty for $P_L(u)$ can be performed [7]. One can see that for most wind speeds the power curve has very little uncertainty. Nevertheless, larger uncertainties occur in the region of transition to rated power. There the power conversion is close to stability over a wider range of power values, as a consequence of the changing control strategy from partial load to full load operation (see Fig. 5). It is a region of great interest as the controller of the wind turbine is highly solicited for the transition to rated power.

3.3.4 Advantages of the Langevin approach

The Langevin equation (24) is a simplifying model for the power conversion process. The question of its validity for wind turbine power signals was positively answered in recent developments [11], as the power signal of a wind turbine could

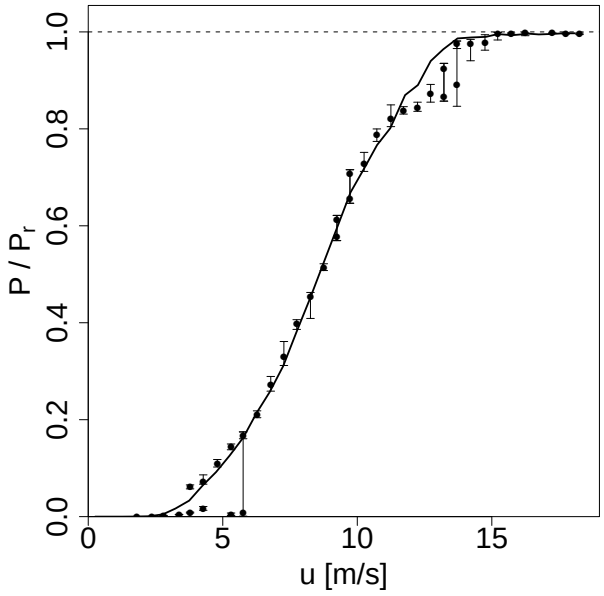

Fig. 15 Langevin power curve (black dots with corresponding error bars) and IEC power curve (solid line).

be successfully modelled. Predicting power signals from the Langevin equation is introduced in appendix 7. Also, the drift function $D^{(1)}$ is well-defined for a large class of stochastic processes, and is not limited only to the class of the Langevin processes.

Also, the definition of the drift function does not suffer the systematic errors caused by temporal averaging. For such, the Langevin power curve characterizes the wind turbine dynamics only, regardless of the wind condition during the measurement[22]. The results are therefore machine-dependent only, and not site- or measurement-dependent, as the intensity of turbulence has no influence on the Langevin power curve.

Additionally, this approach can show complex characteristics of the investigated system, such as regions where the system is close to stability, as mentioned above, or multiple stable states, see also [1, 9]. For these various reasons, the Langevin power curve represents a promising tool for power performance monitoring, as will be introduced in section 4.

[22] Assuming that the measurement period is sufficiently long to reach statistical convergence.

3.4 Power curve stability under different wind measurement technologies

Wind measurements are ordinarily performed using a cup anemometer for the speed and a wind vane for the direction. Yet new techniques appear in wind energy industry as alternatives, such as LIDAR (LIght Detection And Ranging) anemometry[23]. It represents a promising technology for wind measurements as it makes remote measurements possible. This becomes particularly interesting for larger heights, where the efforts for measurement towers reach critical levels. This holds especially for power curve measurement, considering the growing heights of recent wind turbines.

LIDAR measurements presented here are performed using a Leosphere WindCube system. It operates as a pulsed laser Doppler anemometer, see Fig. 16. An infrared laser beam is inclined by approximately 30° against the vertical direction and takes beamwise Doppler measurements of the wind velocity. These measurements are performed in the four principal directions, and a three-dimensional wind vector is then derived from the four most recent measurements. The device achieves a sampling rate of 0.67 Hz. Because of the pulsed laser operation, measurements can be obtained in up to ten height levels simultaneously, within a range between 40 and about 200 m.

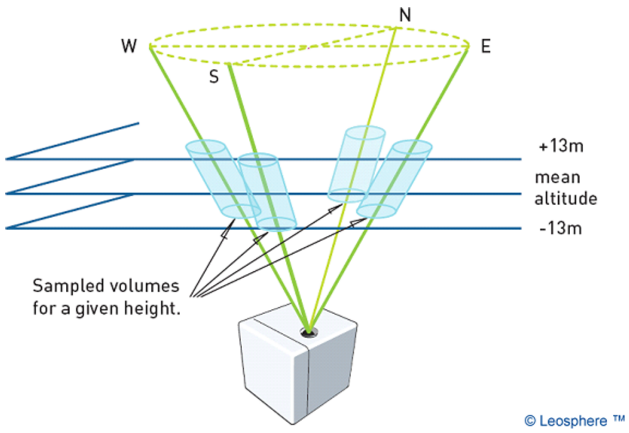

Fig. 16 Operation principle of the Leosphere WindCube. Sketch ©Leosphere, Inc.

Power curve measurements were performed using both LIDAR, cup and ultrasonic anemometers. The measurement was deployed in a distance of 2.5 rotor diameters away from a prototype multi-MW class offshore wind turbine. The temporal resolution of the power data, the wind speed recorded from the cup and ultrasonic anemometers was 1 Hz, while the LIDAR achieved 0.67 Hz. Further details on the

[23] Another alternative is given by ultrasonic anemometers which can estimate at once the wind speed and direction.

measurements can be found in [22]. From these measurement data the IEC and Langevin power curves of the wind turbine could successfully be derived. Figure 17 shows the Langevin power curve from LIDAR wind measurement.

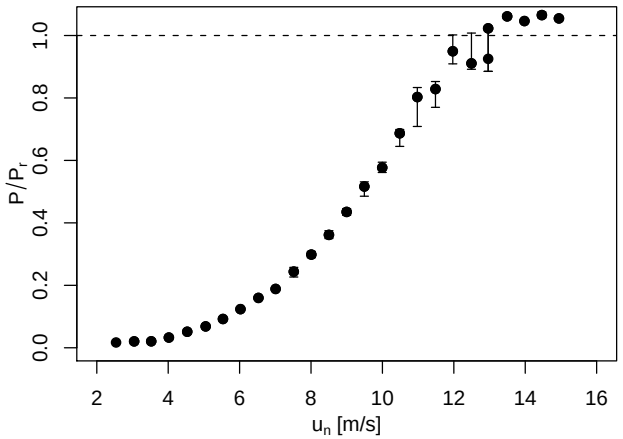

Fig. 17 Langevin power curve of a multi-MW class offshore prototype wind turbine, derived from LIDAR wind measurement [22].

The IEC and Langevin power curves are in excellent agreement when derived from LIDAR, cup and ultrasonic anemometer measurements [22].

For the near future, a substantial increase in the use of wind LIDARs can be expected. These measurements therefore will also open the possibility of precise and uncomplicated derivation of power curves, thanks to the portability of LIDAR devices.

4 Applications - power performance monitoring

Two methods were introduced to estimate power curves in section 3. Because the two methods differ by the time scales they investigate[24], the IEC method is more suited for long-term analysis, while the Langevin method focuses more on short-time dynamics, bringing deeper insight on the inner mechanical behavior. This allows for a complementary assessment of the overall performance.

The two methods also differ by their dimension, as explained in section 4.1. This aspect works constructively with their respective time scales, making the IEC

[24] For reminder, the IEC method focuses on time scales of 10 minutes, while the Langevin approach investigates the dynamics in the order of few seconds.

power curve more suitable for an estimation of annual energy production (AEP), and making the Langevin power curve more suitable to detect dynamical anomalies. These two applications are presented respectively in sections 4.2 and 4.3.

4.1 One-dimensional versus two-dimensional power curves

The two different ways to discretize data brings the most difference between the two different approaches.

The IEC method discretizes the two-dimensional domain $\{u,P\}$ into wind speed bins of size $\delta u = 0.5m/s$. As the domain is discretized only for the wind speed, the IEC power curve depends on its unique variable u, resulting in a unique point every $0.5m/s$. The IEC power curve is hence one-dimensional, it is the line $P_{IEC}(u)$.

However, the Langevin approach discretizes the domain $\{u,P\}$ on both wind speed and power output. The drift function $D_i^{(1)}(P)$ depends on the two variables u_i and P, making $D^{(1)}$ a two-dimensional estimate. This justifies why several stable fixed points are possible for a given wind speed. An example is presented in Fig. 18.

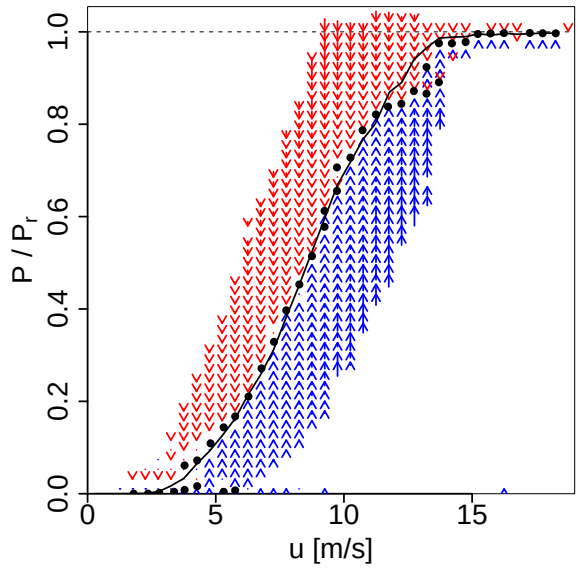

Fig. 18 Drift function $D_i^{(1)}(P)$ (arrows), Langevin power curve $P_L(u)$ (dots) and IEC power curve $P_{IEC}(u)$ (line).

The two-dimensional framework of the Langevin analysis allows to observe local[25] dynamics. An example can be seen in Fig. 18 for $u = 13$m/s, as the wind turbine tends to $P = 0.9 \cdot P_r$ when in partial load operation and to $P = P_r$ when in full load operation. Limited by its unique dimension, the IEC power curve can only display the average value in between. Multi-stable behaviors, created for example by a multiple-gear gearbox, switching generator stages or changing control strategies cannot be resolved by the IEC power curve.

4.2 Annual energy production

The one-dimensional *limitation* of the IEC power curve becomes an advantage for long-term energy production, as $P_{IEC}(u)$ relates unambiguously a unique value of power for each wind speed. As the AEP estimates the energy produced over a year, it can be seen as a prediction estimate. A prediction of power production at high-frequency is also possible using the Langevin approach, as introduced in appendix 7. This is a more complicated approach that is outside the scope of this section.

The estimation of the AEP extrapolates the power production of a wind turbine characterized by its power curve in a given location. This section 4.2 does not give an exact transcription of the AEP procedure from the IEC norm [10], but rather a comprehensive introduction on how power production can be estimated simply from a wind speed measurement. For such, the *AEP procedure* introduced here is not the official AEP procedure following IEC, but a similar version. In both cases, the availability of the wind turbine is assumed to be 100%.

4.2.1 Estimating the wind resource

Any location scheduled to host a wind turbine can be categorized in advance by a characterization of its wind resource. A local measurement of wind speed from a met mast at hub height[26] of the hypothetical wind turbine must be performed, typically over one year[27]. From this wind speed measurement $u(t)$, a ten-minute (or hourly) averaging is applied on $u(t)$. The probability density function (PDF) $f(u_i)$ of the ten-minute average values u_i is established. For clarity, the values u_i will be labelled u. $f(u)$ returns the probability of occurrence of the wind speed u. For long enough measurements, $f(u)$ is known to fit a Weibull distribution [17]

$$f(u;\lambda,k) = \frac{k}{\lambda}\left(\frac{u}{\lambda}\right)^{k-1} e^{(-u/k)^k}, \tag{27}$$

[25] Local in wind speed and power output.

[26] Typical hub heights of commercial multi-MW class wind turbines are in the order of 100m, justifying the interest for a portable LIDAR sensor, see section 3.4.

[27] A measurement of wind speed over one year covers the various wind situations resulting from various seasonal behaviors.

where k and λ[28] are called respectively the shape and scale factors [29]. Visual examples of such wind speed distributions are given in [6].

4.2.2 Estimating the AEP

A given wind site is characterized for the AEP by its wind speed PDF $f(u)$, while a given wind turbine is characterized by its IEC power curve. As P_{IEC} relates unambiguously a given wind speed U to the corresponding average power output $P_{IEC}(U)$, the power curve serves as a transfer function from wind speed to average power output. An estimation of the average power output $\overline{P}$ can be obtained following

$$\overline{P} = \int_0^\infty f(u) \times P_{IEC}(u)\, du\,, \tag{28}$$

and an estimation for the energy production over a period T reads

$$T \times \overline{P} = T \int_0^\infty f(u) \times P_{IEC}(u)\, du\,. \tag{29}$$

Over one year, $T = 8766$ hours and

$$AEP = \overline{P} \times 8766\,, \tag{30}$$

where $\overline{P}$ is given in Watt and AEP is given in Watt hour.

Thanks to its simple mathematical procedure, the AEP is commonly used to make rough predictions of energy production, as well as for financial estimations. It can predict how much energy a wind turbine will generate on a given site before installing it. This allows for an optimal choice of design for the optimal location. This result however remains a rough estimation.

4.3 Detecting dynamical anomalies

The intention of dynamical monitoring is to detect dynamical anomalies that appear on operating wind turbines. Monitoring refers to the time evolution of the power performance here. A good monitoring procedure should be reliable[30], as fast as

[28] One should note here that λ is not the tip speed ratio of a wind turbine, but a parameter of the Weibull distribution.

[29] The IEC norm [10] refers to the Rayleigh distribution, which is a special case of the Weibull distribution for $k = 2$.

[30] An over-sensitive procedure might indicate non-existing anomalies, while an under-sensitive procedure would fail to detect a major malfunction.

available, and possibly also inform on the source of the anomaly. While monitoring procedures come to be ever more complex, the approach presented here is based only on a power curve estimation. This approach is not intended to give a full-featured method, but rather an illustration of the amount of information given by power curves. More advanced studies on the topic of power curves for monitoring are being developed, but remain outside the scope of this introduction as they represent active research topics.

The monitoring procedure simply consists in computing $P_L(u)$ at an initial time that will serve as a reference[31]. Potential changes in time of $P_L(u)$ are considered anomalies, or malfunctions inside the wind turbine that spoil the conversion dynamics. While this strategy is very simple, the challenge lies in defining the right threshold for a change in $P_L(u)$ to be considered an anomaly. This threshold, along with other parameters such as the necessary measurement time or time reactivity of the method depend on the wind turbine design and location.

To illustrate the ability of the method, the monitoring procedure was applied on a numerical simulation. The simulation was applied on measurement data, where an anomaly was introduced. This artificial anomaly limits the power production to $P \approx 0.55 \cdot P_r$ for intermediate wind speeds, as represented by the grey rectangles in Fig. 19 and 20. More clearly, when in this rectangle, the power signal was sometimes forced to reduce towards $0.55P_r$. From this artificial data, $P_L(u)$ and $P_{IEC}(u)$ were then computed and compared to the original data. This is illustrated in Fig. 19 and 20.

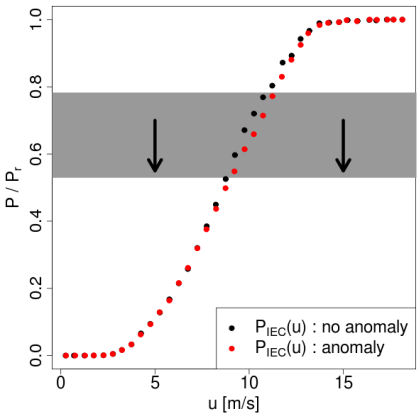

Fig. 19 Comparison of $P_{IEC}(u)$ before the anomaly (black in background) and after the anomaly (grey in front). The artificial anomaly was applied in the grey rectangle.

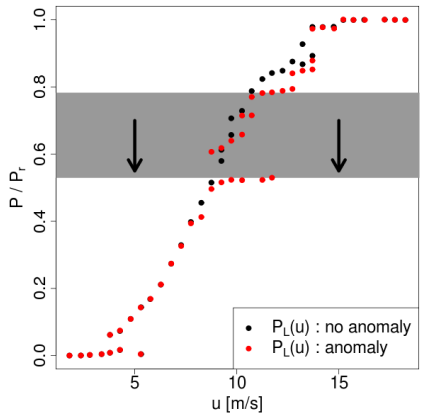

Fig. 20 Comparison of $P_L(u)$ before the anomaly (black in background) and after the anomaly (grey in front). The artificial anomaly was applied in the grey rectangle.

[31] The reference time is chosen when the wind turbine is believed to work with full capacity.

Similar anomalies were observed on several real wind turbines. (justifying the reason for this artificial anomaly). For information, the total energy production was reduced to 96.6% compared to the original energy production due to the presence of the anomaly. Fig. 20 illustrates the higher reactivity of $P_L(u)$. While in Fig. 19 $P_{IEC}(u)$ only shows a minor deviation in the region of the anomaly, $P_L(u)$ clearly *detaches* from the typical cubic curve to adjust to the new dynamics. $P_L(u)$ can detect changes in the dynamics of the conversion process, unlike $P_{IEC}(u)$ that is better suited for the AEP.

The Langevin power curve is more reactive to changes in the dynamics. As the IEC power curve averages over 10 minutes intervals, the information about high-frequency dynamics is lost. Also, the second averaging in wind speed prevents from seeing multi-stable behaviors.

In addition, the Langevin power curve does not depend on the turbulence intensity, unlike the IEC power curve, see section 3.2.3. A deviation in the Langevin power curve indicates a change in the conversion dynamics, regardless of the wind situation. This makes the Langevin power curve a promising tool for dynamical monitoring.

5 Conclusion

This chapter was first dedicated to power performance for wind turbines. A general overview was introduced in section 2, mainly the application of momentum theory to wind turbines, as developed by Betz. This simplified analysis sets an upper limit of $\approx 60\%$ for the power available in the wind, regardless of the design of the wind power system. Additional losses due to more realistic considerations bring an even lower availability for the power extraction, up to $\approx 50\%$ for modern commercial designs. Estimates of power performance like the power coefficient or the theoretical power curve were defined for the case of a laminar wind flow.

Facing complex turbulent and atmospheric effects, wind turbines cannot be described satisfactorily using a laminar theory. Statistical tools were introduced in section 3 to integrate these complex effects into the analysis. The international procedure to estimate a reliable power curve was introduced by the IEC norm 61400-12-1. It sets good guidelines on how to perform measurements on operating wind turbines, and provides a uniform standard. It handles the measured signals of wind speed and power output through an averaging procedure both in time and on the wind speeds. It results an uncomplicated IEC power curve that accounts somewhat for the turbulent effects. Unfortunately, the result depends on the measurement condition, such that the IEC power curve does not characterize the wind turbine performance only, but also the wind condition. This procedure allows however for a gross estimation of long-time energy estimation like the AEP, as introduced in section 4.2.

An alternative is proposed that is based on stochastic analysis. Instead of averaging over time, the power signal is approximated to solve a Langevin equation. A drift function is introduced, that quantifies the reaction dynamics of a wind turbine to turbulent wind fluctuations. It results a so-called Langevin power curve, which represents the stable fixed points of the conversion dynamics. The Langevin power curve and the drift function give a simplified model of how the wind turbine actively adapts the power production to the changing wind speed. Unlike the IEC power curve, the Langevin power curve does not depend on the measurement condition, and characterizes the wind turbine only. Also its two-dimensional structure allows for a more flexible result and can resolve multi-stable dynamics. This makes the Langevin approach a promising application for performance monitoring, as discussed in section 4.3. Modeling of power signals is also made possible through the Langevin equation, as briefly introduced in appendix 7.

As the wind energy industry grows rapidly, wind turbine designs might (or might not) change radically in the next decades. The freedom of change in the overall design is however limited by the physical aspects of the wind itself. The three-blade design emerged as it extracts the most power over the range of wind speeds that occur most often at hub height. Improvements in material engineering allow for larger wind turbines every year. With taller wind turbines, the impact of turbulence induced by the surface roughness of the ground is reduced. This also justifies the recent effort to build offshore wind turbines, that can benefit from smoother winds. Yet the wind remains in essence turbulent, and the wind resource is consequently intermittent. This chapter aimed to identify the response of a single wind turbine to such driving condition. On a larger scale, current challenges involve a smooth integration of a rapidly increasing amount of intermittent wind power into electrical networks. While a single wind turbine is insignificant on the scale of an entire network, a better understanding of single wind turbines, wind parks and global wind installations remains paramount for a future integration of wind energy at a global level.

Acknowledgements Parts of this work have been financially supported by the German Ministry for Environment (BMU) under grant number 0327642A. The authors would like to thank Stephan Barth, Julia Gottschall, Edgar Anahua and Michael Hölling for their pioneering work on the Langevin approach, as well as for stimulating discussions.

References

1. Edgar Anahua, Stephan Barth, and Joachim Peinke. Markovian power curves for wind turbines. *Wind Energy*, 11(3):219–232, 2008.
2. A. Betz. Die windmühlen im lichte neuerer forschung. *Die Naturwissenschaften*, 15:46, 1927.
3. F.D. Bianchi, H. De Battista, and R.J. Mantz. *Wind Turbine Control Systems*. Springer, Berlin, 2nd edition, 2006.
4. F. Böttcher, J. Peinke, D. Kleinhans, and R. Friedrich. Handling systems driven by different noise sources – implications for power estimations. In *Wind Energy*, pages 179–182. Springer, Berlin, 2007.

5. Frank Böttcher, Stephan Barth, and Joachim Peinke. Small and large fluctuations in atmospheric wind speeds. *Stoch Environ Res Ris Assess*, 21:299–308, 2007.
6. T. Burton, D. Sharpe, N. Jenkins, and E. Bossanyi. *Wind energy handbook*. Wiley, New York, 2001.
7. Julia Gottschall. *Modelling the variability of complex systms by means of Langevin processes*. PhD thesis, Carl von Ossietzky Universität Oldenburg, Germany, 2009.
8. Julia Gottschall and Joachim Peinke. Stochastic modelling of a wind turbine's power output with special respect to turbulent dynamics. *Journal of Physics: Conference Series*, 75:012045, 2007.
9. Julia Gottschall and Joachim Peinke. How to improve the estimation of power curves for wind turbines. *Environmental Research Letters*, 3(1):015005 (7pp), 2008.
10. IEC. Wind Turbine Generator Systems, Part 12: Wind turbine power performance testing. International Standard 61400-12-1, International Electrotechnical Commission, 2005.
11. Patrick Milan, Tanja Mücke, Matthias Wächter, and Joachim Peinke. Two numerical modeling approaches for wind energy converters. *Proceedings of Computational Wind Engineering 2010*, 2010.
12. Athanasios Papoulis. *Probability, Random Variables, and Stochastic Processes*. McGraw-Hill, 3rd edition, 1991.
13. W.J.M. Rankine. On the mechanical principles of the action of propellers. *Transactions of the Institute of Naval Architects*, 6:13–39, 1865.
14. A. Rauh and W. Seelert. The Betz optimum efficiency for windmills. *Applied Energy*, 17:15–23, 1984.
15. Alexander Rauh. On the relevance of basic hydrodynamics to wind energy technology. *Nonlinear Phenomena in Complex Systems*, 11(2):158–163, 2008.
16. Alexander Rauh and Joachim Peinke. A phenomenological model for the dynamic response of wind turbines to turbulent wind. *J Wind Eng Ind Aerodyn*, 92(2):159–183, 2004.
17. L. F. Richardson. *Weather prediction by numerical process*. Cambridge University Press, Cambridge, 1922.
18. Hannes Risken. *The Fokker-Planck equation*. Springer, Berlin, 1984.
19. A. Rosen and Y. Sheinman. The average power output of a wind turbine in turbulent wind. *J Wind Eng Ind Aerodyn*, 51:287, 1994.
20. J. Schneemann, P. Knebel, P. Milan, and J. Peinke. Lift measurements in unsteady flow conditions. *Proceedings of the European Wind Energy Conference 2010*, 2010.
21. J. Twele and R. Gasch. *Windkraftanlagen*. Teubner B.G. GmbH, 2005.
22. Matthias Wächter, Julia Gottschall, Andreas Rettenmeier, and Joachim Peinke. Dynamical power curve estimation using different anemometer types. In *Proceedings of DEWEK, Bremen, 26.–27.11.2008*.

6 Appendix 1: aerodynamics of rotor blades

The essential (mechanical) element of a wind turbine is the rotor, that transforms the power of the wind into a rotational or mechanical power. The ideal requirements are:

- the rotation should be steady and smooth;
- dynamical loads should be minimal;
- the regulation should be done without sudden jumps.

The number of blades, their profile and design should guarantee these features. Modern wind turbines rotate due to the lift forces F_L acting on the airfoils. For an airfoil the effective area[32] can be expressed in terms of the depth t and the wingspan b (normally equal to the rotor radius R), such that

[32] This effective area is the one that enters the formula to calculate drag and lift forces.

$$F_D = C_D(\alpha)\frac{1}{2}\rho c^2(t\cdot b)$$
$$F_L = C_L(\alpha)\frac{1}{2}\rho c^2(t\cdot b)\,, \tag{31}$$

where α is the angle of attack, as displayed in Fig. 21. The lift-drag ratio F_L/F_D relates to the quality of the airfoil. The larger the ratio, the better the quality.

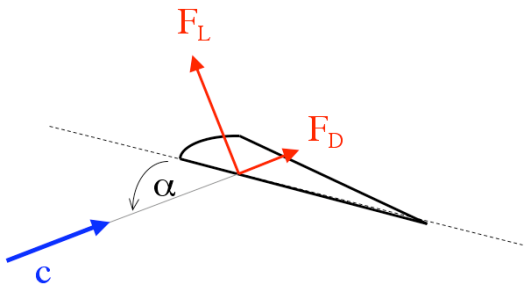

Fig. 21 Cut through an airfoil to illustrate the forces acting on it. The depth t is given by the distance between the leading and the trailing edge. The wingspan b is the length of the airfoil, here perpendicular to the illustrated plane.

In Fig. 21, the velocity vector $\mathbf{c}$ gives the wind velocity in the frame of reference of the airfoil. The wind velocity is $\mathbf{u_2}$ in the frame of the ground, but the rotational motion of the rotor must be considered for the motion of the wind with respect to the blades. Hence, $\mathbf{c}$ is the superposition of the horizontal axial velocity $\mathbf{u_2}$[33] and of the rotational velocity $v = \omega r$, such that

$$c^2(r) = (2u_1/3)^2 + (\omega r)^2\,. \tag{32}$$

The rotor *feels* the effective wind speed $\mathbf{c}$. This is illustrated in Fig. 22.

Instead of integrating the lift and drag forces on the entire airfoil, one can estimate the local force on each infinitesimal element. Also, the total force is divided into its rotational component F_r and its axial component F_a. Considering a cut dr at r in the polar plane of the rotor, the resulting force is

$$F_r = \frac{\rho}{2}c^2\cdot t\cdot dr\,[C_L cos(\beta) - C_D sin(\beta)]$$
$$F_a = \frac{\rho}{2}c^2\cdot t\cdot dr\,[C_L cos(\beta) + C_D sin(\beta)]\,. \tag{33}$$

Also, on can estimate

$$tan(\beta) = \frac{\omega r}{u_2} = \frac{\omega R}{u_1}\frac{r}{R}\frac{u_1}{u_2} = \frac{3}{2}\lambda\frac{r}{R}\,. \tag{34}$$

The idea is to construct the blades in such a way that for each radial annulus they extract the (Betz) optimal power out of the wind

$$F_{r,Betz} = \frac{16}{27}\cdot\frac{\rho}{2}\cdot u_1^3\cdot(2\pi r dr)\,. \tag{35}$$

[33] For the Betz optimum, $u_2 = 2/3u_1$.

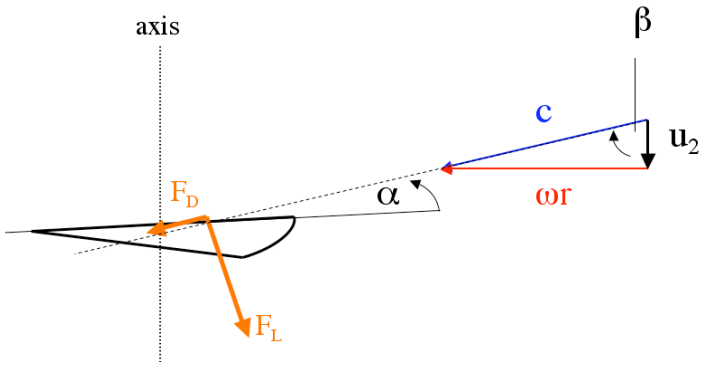

Fig. 22 Cut through a rotating airfoil. The rotational velocity ωr is perpendicular to the axial velocity vector $\mathbf{u_2}$. β denotes the angle between the resulting velocity $\mathbf{c}$ and the rotational direction.

This power also reads

$$dP = z \times F_r \times \omega r\,, \tag{36}$$

where z denotes the number of blades, ωr the velocity in rotational direction and F_r the force in this direction[34]. Inserting equation (33) and combining equations (35) and (36), the optimal value of the depth t as a function of r can be determined. Assuming that $C_D \ll C_L$ and a sufficiently large tip speed ratio (for details see [21]), the profile of the airfoil $t(r)$ reads

$$\begin{aligned} t(r) &\approx \frac{16\pi}{9}\frac{R^2}{zC_L r\lambda^2} \\ &\propto z^{-1}\cdot C_L^{-1}\cdot r^{-1}\cdot\lambda^{-2}\,. \end{aligned} \tag{37}$$

This has an important consequence on the design of rotor blades. The depth decreases with increasing number of blades, larger lift coefficient, increasing radius and especially increasing tip speed ratios. This explains why fast rotating wind turbines tend to have only two or three narrow blades while old western-mill machines have many, rather broad blades.

7 Appendix 2: a relaxation model for the power output

As introduced in section 3.3.2, the power output of wind turbines is assumed to be solution of a Langevin equation

$$\frac{d}{dt}P(t) = D^{(1)}(P) + \sqrt{D^{(2)}(P)}\times\Gamma(t)\,. \tag{38}$$

For reminder, the power value P and the functions $D^{(1)}$ and $D^{(2)}$ are conditioned on the wind speed bins, as done in the main text. The subscript $_i$ indicating the wind speed bin was dropped for simplicity. $D^{(1)}$ represents the deterministic dynamics of the conversion process, that always push the power output towards the Langevin power curve $P_L(u)$. Additional random fluctuations

[34] The force in the axial direction does not contribute to the power production of a wind turbine but to the thrust on it.

are superposed as a simplified model for all the microscopic degrees of freedom acting on the conversion process[35]. A simple but rather realistic ansatz for $D^{(1)}$ would be

$$D^{(1)}(P) = \alpha \left(P_{theo}(u) - P(t) \right) , \tag{39}$$

where $D^{(1)}$ linearly drives the power output towards the instantaneous value of the theoretical power curve $P_{theo}(u(t))$, which might read

$$P_{theo}(u) = \begin{cases} P_r \left(\frac{u}{u_r} \right)^3 & \text{for } u < u_r \, , \\ P_r & \text{for } u \geq u_r \, . \end{cases} \tag{40}$$

Assuming equation (39) and a constant diffusion function $D^{(2)}(P) = \beta$[36], the Langevin equation becomes a relaxation model for the power output

$$\frac{d}{dt} P(t) = \alpha \left(P_{theo}(u(t)) - P(t) \right) + \sqrt{\beta} \times \Gamma(t) \, . \tag{41}$$

Equation (41) is a phenomenological model for the power signal. This special case of the Langevin process is mathematically called an Ornstein-Uhlenbeck process [18].
Equation (41) is a simplified model for the power output, where the wind turbine design is described through the parameters α and β, as well as the power curve $P_{theo}(u)$. The parameter α is related to the reaction time of the model wind turbine[37] , while β quantifies the strength of the stochastic noise. $\Gamma(t)$ is a Gaussian-distributed white noise with mean value 0 and variance 2, which can be generated easily from most mathematical softwares. Using a wind speed time series $u(t)$ as an input for the model equation[38], a time series of power output $P(t)$ can be generated at the same sampling frequency. An example is provided in Fig. 23.
From Fig. 23, it can be seen that the relaxation model manages to estimate the power output of a wind turbine to a first approximation. Fluctuations and their statistics are more difficult to reproduce than long-time behavior, which is mostly driven by the changes in wind speed rather than by the stochastic fluctuations. More advanced methods are being developed, as introduced in [11], where $D^{(1)}$ and $D^{(2)}$ are not assumed but estimated from measurement data.

[35] The Langevin equation relates directly the incoming wind speed and the power output. Many other variables are involved in intermediate steps of the conversion, which should be modeled by a set of mutli-dimensional deterministic differential equations. All these degrees of freedom are modeled by the one-dimensional stochastic Langevin equation instead.

[36] A constant diffusion function yields additive noise. More complex systems such as turbulence-driven systems display multiplicative noise and a non-constant diffusion function.

[37] A realistic model integrates a finite reaction time due to the inertia of the wind turbine to changing wind speeds.

[38] An initial condition $P(t = 0)$ for the power output is also necessary. However, the result depends only poorly on this value, as the dynamics will adjust rapidly to the given wind speed.

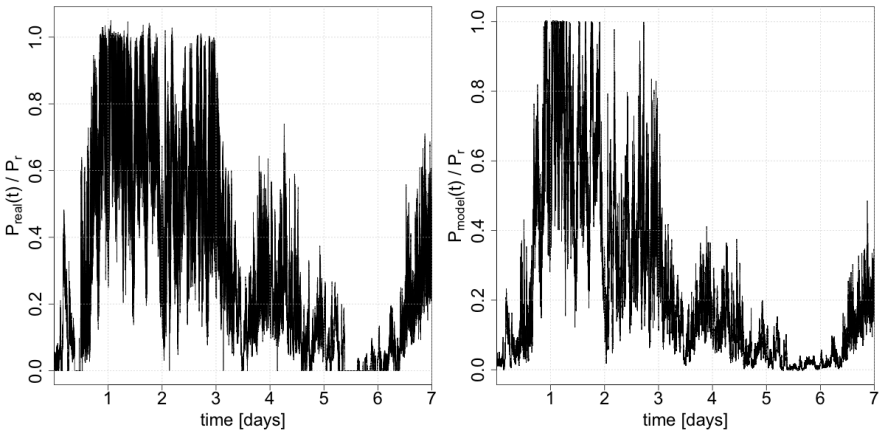

Fig. 23 (a) Power signal measured. (b) Power signal modeled following equation (41) with $\alpha = 0.005$, $\beta = 0.5$, $u_r = 13$ m/s and $P_r = 1$. The wind speed signal used was measured simultaneously as the measured power output.